JGR Space Physics

RESEARCH ARTICLE
10.1029/2019JA027508

Another Mini Solar Maximum in the Offing: A Prediction for the Amplitude of Solar Cycle 25

S. K. Bisoi[1], P. Janardhan[2], and S. Ananthakrishnan[3]

[1]Key Laboratory of Solar Activity, National Astronomical Observatories, Chinese Academy of Sciences, Beijing, China, [2]Physical Research Laboratory, Astronomy & Astrophysics Division, Ahmedabad, India, [3]Electronics Science Department, Pune University, Pune, India

Key Points:
- Cycle 25 will be stronger than cycle 24
- A reduced floor level of heliospheric magnetic field in the minimum of cycle 24
- Anti-correlation of unsigned polar magnetic fields with solar cycle in cycle 24

Correspondence to:
S. K. Bisoi,
susanta@nao.cas.cn

Citation:
Bisoi, S. K., Janardhan, P., & Ananthakrishnan, S. (2020). Another mini solar maximum in the offing: A prediction for the amplitude of solar cycle 25. *Journal of Geophysical Research: Space Physics*, *125*, e2019JA027508. https://doi.org/10.1029/2019JA027508

Received 9 OCT 2019
Accepted 21 MAR 2020
Accepted article online 11 JUN 2020

Abstract We examine the temporal changes in both solar polar magnetic field (PMF) at latitudes ≥45° and heliospheric magnetic field (HMF) at 1 AU during solar cycles 21–24 with emphasis on the recent activity changes after July 2015, the so called "mini solar maximum" of cycle 24. While unsigned PMF shows solar cycle modulations in cycles 21 and 22, it shows an anti-correlation with solar cycle variation in cycle 24. In addition, the floor level of the HMF (of 4.6 nT), that is, the value that the HMF returns to at each solar minimum, is breached about 2 years prior to cycle 24 minimum, indicating a reduced HMF floor level of 3.2 ± 0.5 nT in the upcoming cycle 24 minimum. In light of the change of unsigned PMF and the availability of a revised smoothed sunspot number (SSN V2.0) after July 2015, we revisit the correlation of unsigned PMF and HMF at solar minimum. The correlation is used to estimate values of the HMF at the cycle 24 minimum and the amplitude of the upcoming cycle 25. The updated prediction is 134 ± 11 or 131 ± 11 on the revised SSN V2.0 scale assuming the cycle 24 minimum to occur in 2020 or 2021, respectively. The SSN values indicate that the cycle 25 will be stronger than cycle 24 and a little weaker than cycle 23, even if the current solar cycle minimum occurs in 2021 instead of 2020. This implies that we will witness another mini solar maximum in the upcoming cycle 25.

1. Introduction

The solar cycle activity that waxes and wanes with a period of 11 years modulates the heliospheric environment and has potential implications for changes in "space weather." It is, therefore, extremely important to understand long-term changes in solar cycle activity and to accurately predict the behavior of upcoming solar cycles. A number of satellites and space missions in the recent years, including many being planned for the future, also require knowledge of future solar cycle activity in planning the missions properly.

The current solar cycle 24 is the fourth successive cycle, since cycle 21, in a continuing trend of diminishing sunspot cycles. It is also one of the weakest cycles, since cycle 14, with a peak smoothed sunspot number (SSN) of only 116 in the revised sunspot scale. The maximum of solar cycle 24 has therefore dubbed as the "mini solar maximum." Recent studies have also claimed that the Sun in the future may move into a period of very low sunspot activity comparable with the Dalton (Zolotova & Ponyavin, 2014) or even the Maunder minimum (Sánchez-Sesma, 2016; Zachilas & Gkana, 2015).

This unusual behavior has drawn the attention of researchers worldwide who have attempted to predict the amplitude of solar cycle 25 (Bhowmik & Nandy, 2018; Cameron et al., 2016; Gopalswamy et al., 2018; Hathaway & Upton, 2016; Iijima et al., 2017; Janardhan et al., 2015; Jiang et al., 2018; Kakad et al., 2017; Kirov et al., 2018; Macario-Rojas et al., 2018; Pesnell & Schatten, 2018; Petrovay et al., 2018; Sarp et al., 2018; Upton & Hathaway, 2014, 2018). The different estimates of SSN in V1.0 and V2.0 for the amplitude of cycle 25 by different researchers along with the ratio of peak SSN of cycle 25 to cycle 24 are summarized in Table 1. It is to be, however, noted from Table 1 that the solar cycle 25 predictions made prior to 2017, except that for Kirov et al. (2018), usually used the unrevised SSN observations, referred to henceforth as SSN V1.0, while the solar cycle 25 predictions made after 2017 mostly used the SSN V2.0 observations. It must be clarified here that as of July 2015 a revised and updated list of the (Wolf) sunspot numbers has been adopted, referred to as SSN V2.0 (Clette & Lefèvre, 2016; Cliver, 2016). In our previous solar cycle prediction (Janardhan et al., 2015), abbreviated henceforth as JBA15, a peak SSN of ~62 ± 12 was reported for the amplitude of the upcoming solar cycle 25. For that prediction, we had used the original SSN V1.0 observations, with data for the period 1975–mid-2014. It is also evident from Table 1 that while the predictions made using SSN

Table 1
Estimates of the Amplitude of SSN for Cycle 25 as Reported by Different Researchers

Authors	SSN_{max} (V1.0)	SSN_{max} (V2.0)	$\frac{SSN25}{SSN24}$
Upton and Hathaway (2014)	—	—	≁1
Janardhan et al. (2015)	62 ± 12	-	0.83
Cameron et al. (2016)	—	—	1
Hathaway and Upton (2016)	—	—	1
Kakad et al. (2017)	63 ± 11.3	-	0.84
Iijima et al. (2017)	—	—	<1
Kirov et al. (2018)	50–55	—	0.73
Pesnell and Schatten (2018)	—	135 ± 25	1.16
Jiang et al. (2018)	—	125 ± 32	1.08
Upton and Hathaway (2018)	—	110.6	0.95
Petrovay et al. (2018)	—	130	1.12
Gopalswamy et al. (2018)	—	—	≁1
Macario-Rojas et al. (2018)	—	99.6	0.86
Sarp et al. (2018)	—	154 ± 12	1.32
Bhowmik and Nandy (2018)	—	118	1.01
This study	83 ± 8	134 ± 11	1.00, 1.14

V1.0 observations claimed a weaker cycle 25 than cycle 24 or a similar cycle 25 like cycle 24, the predictions made using SSN V2.0 observations claimed a weaker or stronger cycle 25 than cycle 24 as well as a similar cycle 25 like cycle 24. We therefore revisit, in this paper, our earlier prediction in order to update the amplitude of solar cycle 25 using the revised SSN V2.0 observations available after July 2015 and to find out the nature of solar cycle 25. Pesnell (2018) also suggested that the solar cycle 25 predictions which used the SSN V1.0 observations need to be revisited as he showed that the revised SSN V2.0 observations have different values of SSN for the solar maxima and minima compared to the original SSN V1.0 observations.

Further, we primarily claimed, in our earlier prediction (JBA15), a possible continuation of a steady declining trend observed in unsigned solar polar fields above latitudes of ≥45° starting from ~1995 until the minimum of cycle 24. Taking this trend into account, we estimated a value of unsigned polar field and subsequently a value of heliospheric magnetic field (HMF) in 2020, that is, at the expected minimum of cycle 24. The HMF value was then used as a precursor for predicting the peak SSN of cycle 25. The study (JBA15) used solar photospheric magnetic fields (SPF) data covering the period 1975–mid-2014. Since then, we now have three additional years of observations (up to the current data set of December 2017) of SPF. Recently, Ingale et al. (2019) have claimed that the over 20 year steady decline in unsigned polar fields reported in JBA15 showed an abrupt rise after July 2015 instead of a continuing declining trend. In this paper, we have shown that this change in the declining trend of unsigned polar fields observed after July 2015 would affect the estimated value of unsigned polar fields at the upcoming minimum of solar cycle 24 as obtained in JBA15 and in turn our estimate of the amplitude of cycle 25.

In addition, sunspot numbers data going back over the past 1,000 solar cycles or ~11,000 years in time using ^{14}C records from tree rings have been used to identify 27 grand or prolonged solar minima (Usoskin et al., 2007), implying that appropriate conditions can exist on the Sun to induce grand minima. Choudhuri and Karak (2012) and Karak and Choudhuri (2013) used a flux transport dynamo model to characterize the onset of grand minima seen in this ~11,000 years long data set and reported that one or two solar cycles before the onset of grand minima, the cycle period tends to become longer. There is also evidence of longer cycles before the start of the Maunder and Spörer minimum (Miyahara et al., 2010). Given these conclusions and the fact that the declining trend in photospheric magnetic fields is still continuing (Sasikumar Raja et al., 2019), it is reasonable to raise the question about the peak SSN of cycle 25 if the oncoming solar minimum of cycle 24 were to be delayed, that is, whether it would take place in 2021 instead of 2020 as expected. Upton and Hathaway (2018) also claimed that we may not reach the cycle 24 minimum until 2021. Thus, in this study, we re-estimate the amplitude of solar cycle 25 assuming the minimum of cycle 24 to occur in 2020 or 2021. Importantly, we discuss the variations of unsigned polar fields and HMF after July 2015 which

Table 2
Estimates of the Peak Values of SSN for Solar Cycles 14–24 in V1.0, V2.0, and the One Used by Cliver and Ling (2011)

Solar cycles	SSN_{max} (V1.0)	SSN_{max} (V2.0)	SSN_{max} (Cliver & Ling, 2011)
Cycle 14	64.2	107.1	77.0
Cycle 15	105.4	175.7	126.5
Cycle 16	78.1	130.2	93.7
Cycle 17	119.2	198.6	143.0
Cycle 18	151.8	218.7	151.8
Cycle 19	201.3	285.0	201.3
Cycle 20	110.6	156.6	110.6
Cycle 21	164.5	232.9	164.5
Cycle 22	158.5	212.5	158.5
Cycle 23	120.8	180.3	120.8
Cycle 24	81.9	116.4	-

reveal some new findings that are crucial in the context of recent changes in the Sun's global magnetic field behavior.

2. Data and Methodology

2.1. Smoothed Sunspot Number

For SSN, we used both SSN V1.0 and V2.0 observations obtained from the Royal Observatory of Belgium, Brussels (http://www.sidc.be/silso/data-files). The original version SSN V1.0 was created in 1849 by R. Wolf who derived the daily total sunspot number by the formula: $R_z = Ns + 10 \times Ng$, where Ns is the number of sunspots and Ng is the number of sunspot groups. The original version is maintained at Zurich observatory, while a recalibrated SSN V2.0 version was devised after July 2015 and is maintained by the Royal Observatory of Belgium. Observations of the SSN V1.0 and V2.0 are available since 1749, covering solar cycles 1–24. In our earlier prediction, in JBA15, we directly employed the correlation equation, proposed by Cliver and Ling (2011), between the HMF at solar minimum (B_{min}) of the preceding cycle (n-1) and the peak value of sunspot number smoothed over a period of 13-month (SSN_{max}) of the next cycle (n). Based on the correlation between B_{min} and SSN_{max}, Cliver and Ling (2011) reported a correlation equation given by

$$SSN_{max} = 63.4 \times B_{min} - 184.7 \quad (1)$$

For the correlation, the HMF and the peak values of SSN V1.0 obtained from the National Oceanic and Atmospheric Administration Geophysical Data Center for solar cycles 14 to 23 were used by Cliver and Ling (2011). On the other hand, in this study, we preferred to use SSN V1.0 (blue curve in Figure 1) and V2.0 (red curve in Figure 1) observations from the Royal Observatory of Belgium, Brussels, and that too only from cycles 14–24. It is apparent from Figure 1 that there is no large change observed in temporal variation of SSN V2.0 except for the V2.0 values being about 40–70% higher than V1.0. Also, there is no simple scaling factor between V1.0 and V2.0 that could be used for re-calculation of the predicted peak SSN of solar cycle 25. We have therefore obtained the peak values of SSN in V1.0 and V2.0 during the solar maxima of cycles 14–24 and listed them, respectively, in the second and third columns along with the peak SSN values used by Cliver and Ling (2011) in the fourth column of Table 2. It is now clear from Table 2 that the peak SSN values for solar cycles 14–24 in the two versions have different values. Also, from a comparison of the SSN values in second and fourth columns of Table 2, it is clear that the peak SSN V1.0 used in this study for cycles 14–17 are not in agreement with the peak SSN V1.0 used by Cliver and Ling (2011). We thus used the SSN V1.0 observations from the Royal Observatory of Belgium, in this paper, in order to update the correlation between B_{min} and SSN_{max} as derived by Cliver and Ling (2011). Also, we used the updated SSN V2.0 observations to derive a new correlation equation between B_{min} and SSN_{max}. Consequently, we used these correlation equations to update the prediction for the amplitude of cycle 25 that was made earlier in JBA15.

2.2. Solar Photospheric Fields (SPF)

The SPF, for this study, were computed using medium-resolution line-of-sight (LOS) synoptic magnetograms from the National Solar Observatory, Kitt Peak (NSO/KP) and the Synoptic Optical Long-term Investigations of the Sun (NSO/SOLIS) facilities. Each synoptic magnetogram is available in standard FITS format and represents one Carrington rotation (CR) or 27.2753 day averaged SPF in units of Gauss. The synoptic magnetograms used here were from February 1975 to December 2017, covering CR 1625–CR 2197 and spanning solar cycles 21–24. We computed the unsigned values of SPF in the latitude range 45°–78°, referred to here as polar magnetic fields (PMF). Details about the computation of PMF can be further referred to in Janardhan et al. (2018).

In order to estimate the solar polar fields researchers have, instead, used other different latitude ranges such as, poleward of 45° (Bisoi et al., 2014; Janardhan et al., 2010), 55° (Wilcox Solar Observatory [WSO] polar fields and Janardhan et al., 2018), 60° (de Toma, 2011; Gopalswamy et al., 2012, 2016; Sun et al., 2015), and 70° (Muñoz-Jaramillo et al., 2012). It must be noted that a few researchers used the signed values of

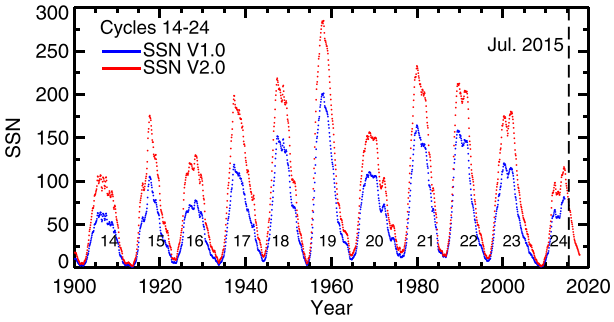

Figure 1. A comparison between the monthly SSN V1.0 (blue) and the monthly SSN V2.0 (red) observations for solar cycles 14–24. The recalibrated SSN V2.0 data are now internationaly used for SSN observations after July 2015.

polar fields for PMF studies, while other researchers preferred the unsigned or total polar fields. In the present study, the unsigned values of NSO polar fields in the latitude range 45°–78° have been used. Janardhan et al. (2018) showed that the overall temporal behavior of NSO polar fields is found to be similar whether one considers the latiude range poleward of 45°, 55°, or 60°. Therefore, in this study, we considered only the solar polar fields in the latitude range poleward of 45°. Also, it is to be noted that one of the poles of the Sun is not clearly visible due to the inclination of the Earth's orbit to the Sun's equator. The polar field data from NSO is therefore corrected for this effect. However, we preferred to compute the solar polar fields leaving out the pole-most regions above the latitude range 78°.

In addition to the unsigned values, we also used the signed values of NSO polar fields in the latitude range 45°–78° in order to compare them with the signed values of WSO polar fields. The WSO polar fields used are actually the 1.58 year filtered LOS PMF obtained from the WSO (https://wso.stanford.edu/Polar.html). The 1.58 year filter is generally used in order to eliminate the yearly geometric projection effects at the poles arised due to the rotation of Earth on the measured LOS fields. The signed values of polar fields were estimated by taking into account the actual magnetic field values, while the unsigned values of polar fields were the absolute of the actual magnetic field values. The unsigned magnetic field value in a particular latitude range actually represents the total photospheric magnetic fields in that latitude range.

The WSO polar fields are considered to be more reliable than the NSO polar fields. Therefore, the NSO polar fields are cross-calibrated with respect to the WSO polar fields so as to find a normalization factor. Figure 2 shows the correlation of NSO polar fields with WSO polar fields. The temporal comparison of NSO and WSO polar fields (figure not shown here) indicate that the NSO polar fields show more deviations from the WSO polar fields in solar cycle 21, while during cycles 22–24, the deviation between the NSO and WSO polar fields is less. Therefore, we plotted the correlation of NSO and WSO polar fields for cycle 21 in Figure 2a and that for cycles 22–24 in Figure 2b. The linear fits give the relations between the two fields, $\mathrm{PMF}_{WSO} = 0.05 + 0.40\ \mathrm{PMF}_{NSO}$ and $\mathrm{PMF}_{WSO} = -0.07 + 0.24\ \mathrm{PMF}_{NSO}$. The Pearson's correlation coefficients, r, are found to be 0.89 and 0.95, respectively. The significance of the correlation was tested using the null hypothesis of a t-test statistics and a P-value (P) of 99%, representing the confidence level, was computed taking into account the r and the sample size, n. The correlations are found to be statistically significant. The values of r, P, and n are indicated at the top left corners of Figures 2a and 2b. Further, we normalized the signed and unsigned NSO polar fields using these linear relations so as to correct for the deviations observed in NSO polar fields with respect to WSO polar fields.

2.3. Heliospheric Magnetic Field (HMF)

We used daily measurements of HMF obtained from the OMNI2 database at 1 AU (https://omniweb.gsfc.nasa.gov/) covering the period February 1975–December 2017 that span solar cycles 21–24. CR-averaged values of HMF were derived in order to compare and correlate them with CR-averaged polar fields during solar cycle minima. We used CR-averaged values for 1 year intervals around solar minima of cycles 20–23 (Wang et al., 2009) corresponding to CR 1642–1654, CR 1771–1783, CR 1905–1917, and CR 2072–2084, respectively.

3. Results

3.1. Polar Magnetic Field (PMF)

Figure 3a plots the cross-calibrated NSO signed PMF in the latitude range of 45°–78° for the period February 1975–December 2017, covering solar cycles 21–24. We have then smoothed the NSO signed PMF with a 13-month running mean and overplotted it as shown by a solid red curve. While for comparison, we have also overplotted the signed WSO PMF (solid black curve) for the period April 1976–April 2019, covering solar cycles 21–24. After the cross-calibration of NSO fields with respect to WSO fields, it is now seen from Figure 3a that the overall temporal behavior of NSO signed PMF during solar cycles 21–24 show a good

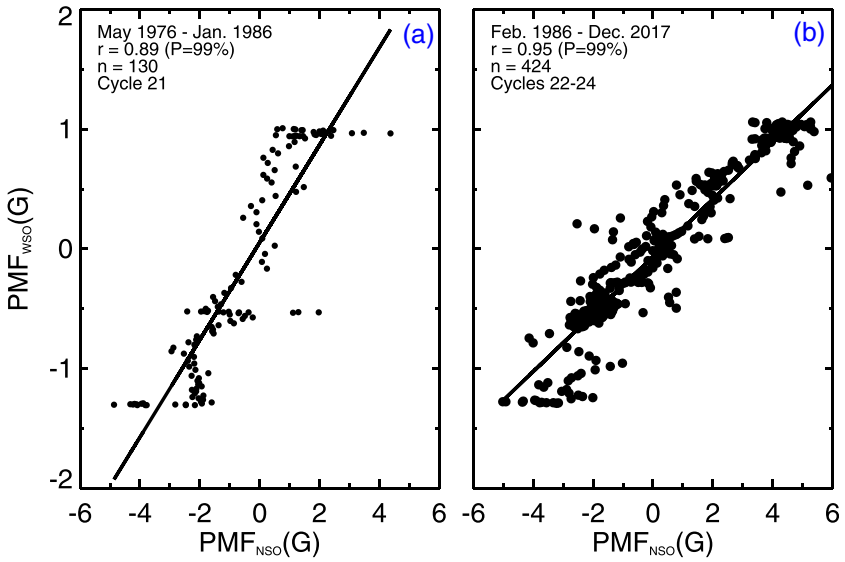

Figure 2. (a) PMF_{WSO} as function of PMF_{NSO} shown for the period May 1976–January 1986 covering solar cycle 21. (b) PMF_{WSO} as function of PMF_{NSO} shown for the period February 1986–December 2017 covering solar cycles 22–24. The filled black dots shown in both panels are data points for the above-mentioned periods, while the solid black lines are overall fits to the respective data points. The values of $r = 0.89$ and $r = 0.95$ are indicated in the top left corners of the panels along with $n = 130$ and $n = 424$, respectively.

agreement with the WSO signed PMF. The signed PMF in each solar cycle shows a maximum strength at the start of the cycle, while at solar cycle maximum, it runs through zero and changes the sign of the field. This is known as reversal of PMF or polar reversal. Subsequently, the signed PMF again shows a maximum strength during the minimum of the cycle. Thus, typically, the signed PMF shows a behavior anti-correlated with solar cycle variation. In cycle 24, after the zero-crossing or reversal of PMF, the signed PMF shows a clear rise in field strength in the year 2015 after solar cycle maximum. Thereafter, it shows a nearly constant value for the next 2 years in the year, that is, 2016 and 2017. The steady value of signed PMF is evident up to April 2019, about 1 year prior to the solar minimum of cycle 24, from the variations of WSO signed PMF. It is to be noted that based on zonal and meridional flow patterns during solar cycles 23 and 24, Komm et al. (2018) estimated that cycle 25 will begin in early 2020. Similar steady values of signed PMF few years before the minimum of the solar cycle can also be seen during earlier solar cycles, that is, cycles 22 and 23. Thus, besides the typical anti-correlation of the signed PMF with solar cycle activity in each solar cycle it also shows a steady value or a polar field plateau prior to the minimum of the solar cycle.

Figure 3b plots the NSO unsigned PMF in the latitude range of 45°–78° for the period February 1975–December 2017, covering solar cycles 21–24. It is evident from a careful examination of the strength of the unsigned PMF (see the solid red curve), referred to henceforth as B_p, that unlike the signed PMF the unsigned PMF shows a totally different temporal behavior. The unsigned PMF shows sunspot cycle like modulations in cycles 21 and 22, while, in cycle 23, no such sunspot cycle like modulation is seen. However, we see a steady decline in the field strength since the start of cycle 23 until the end of cycle 23. Again, at the start of solar cycle 24, in the years 2010 and 2011, there was an increase in the B_p. The annual mean for the years 2010 and 2011 is shown by open black circles. After 2011, the B_p again declined from 2012 up to 2014, only to increase again in the year 2015 after the solar maximum of cycle 24 and has been constant since then. Thus, in contrast to the behavior in previous cycles, the value of B_p, in cycle 24, shows a behavior anti-correlated with solar cycle and a polar field plateau just like the signed PMF, with a maximum strength at the start of the cycle attaining a minimum strength around the solar cycle maximum and again showing a rise in strength after the solar cycle maximum and thereafter attaining a steady value.

We further investigate whether the unexpected rise of B_p during the year 2015 and the subsequent constant value for the next 2 years would change the declining trend. As seen in the years 2010 and 2011, we have already witnessed a rise in the strength of PMF, but the declining trend of the PMF continued after 2011. Hence, we believe that the break in the declining trend during 2015–2017 could be temporary and that

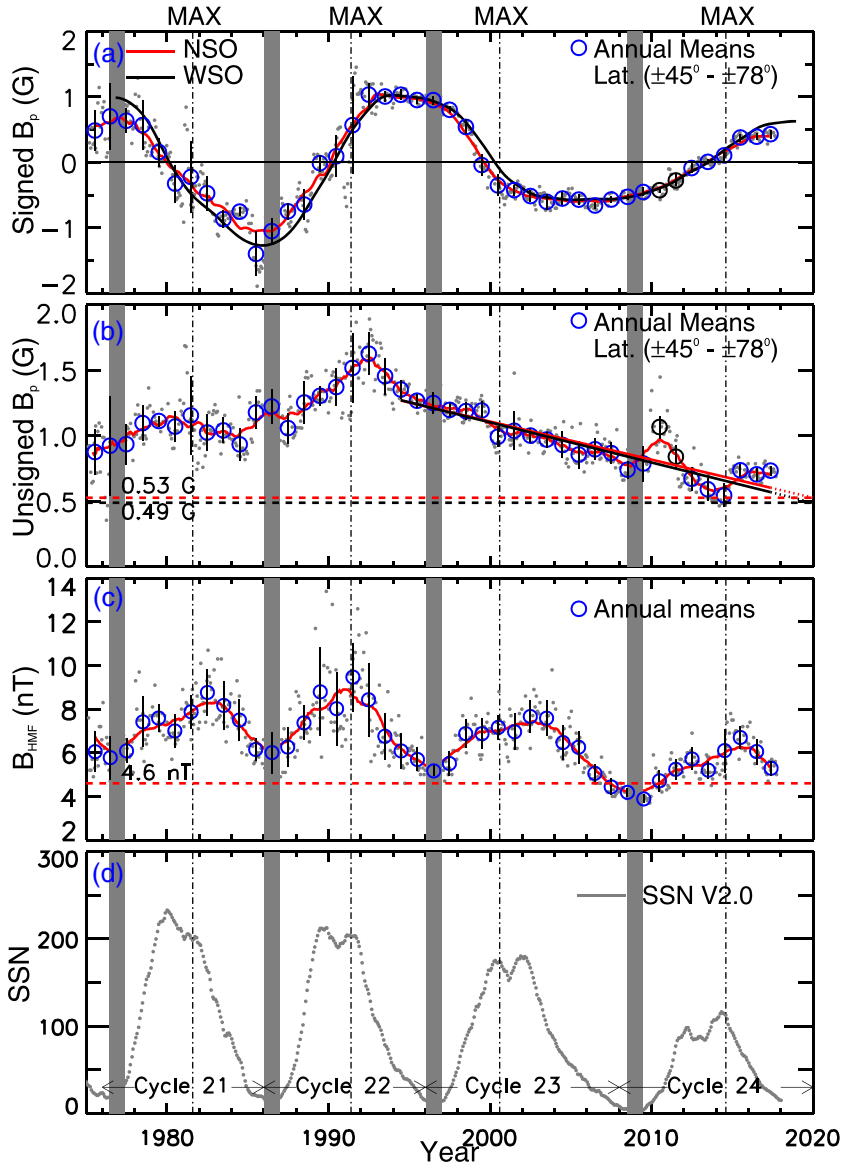

Figure 3. (a) Variations of NSO signed PMF for the time period February 1975–December 2017. Overplotted in solid red curve are smoothed NSO fields while in solid black curve is WSO signed PMF. (b) Variations of NSO unsigned PMF for the same time period as in (a). The solid red and black lines are best fits to the declining trend for the annual means, while the dotted red and black lines are extrapolations of the best fits until 2020. The solid red line is the best fit to all the annual means, while the solid black line is the best fit to all the annual means except for the years 2010 and 2011. The horizontal red and black dashed lines are marked at 0.53 G and 0.49 G. (c) Measurements of HMF during the same period. The horizontal red line indicates the floor level of the HMF of 4.6 nT as proposed by Svalgaard and Cliver (2007). (d) Plotted is the monthly averaged SSN V2.0 data. The filled gray dots, in the top three panels, are CR measurements of SPF, while the open blue circles are annual means with 1σ error bars. The vertical gray bands in each panel demarcate 1 year intervals around the minima of solar cycles 20–23, while the vertical dotted lines in each panel mark the solar maxima of cycles 21–24.

the declining trend may continue. However, the increase in the B_p could affect its rate of decline, and thus change its expected value in 2020, that is, at the expected minimum of cycle 24. We, therefore, re-estimate the value of B_p in 2020 assuming a continuing declining trend. The solid red line in Figure 3b is a least squares fit to the declining trend of B_p for all the annual means in the period 1995–2017, while the broken red line is the extrapolation until 2020. The least squares fit is statistically significant with $r = -0.91$, at a significance level of $P = 99\%$. Similarly, the solid black line in Figure 3b is a least squares fit to the declining trend for all the annual means, with the years 2010 and 2011 being left out, and the broken black line is an extrapolation until 2020. The fit is statistically significant with $r = -0.94$, at a significance

level of $P = 99\%$. The expected values of B_p in 2020 for the above two cases are ~0.53 (±0.02) G and ~0.49 (±0.02) G, as indicated by the dashed horizontal lines in red and black, respectively, in Figure 3b. Thus, the average expected value of B_p in 2020 would be ~0.51 (±0.03) G. The expected values of B_p would be ~0.50 (±0.02) G and ~0.46 (±0.02) G if the solar minimum of cycle 24 is in 2021 instead. Thus, the average expected value of B_p in 2021 would be ~0.48 (±0.03) G.

3.2. Heliospheric Magnetic Field (HMF)

Figure 3c plots the strength of HMF (B_{HMF}) at 1 AU for the period February 1975–December 2017, covering cycles 21–24. A global reduction in the B_{HMF} from solar cycle 22 through solar cycle 23 to solar cycle 24 is evident from Figure 3c. Also, it is seen from Figure 3c that the HMF returns to an average value at each solar minimum, which is known as the floor value of HMF. The floor level of HMF is essentially determined by the baseline flux from the slow solar wind flows. Svalgaard and Cliver (2007) estimated the floor level of 4.6 nT for HMF, indicated by a horizontal red line in Figure 3c, from a correlation of B_{HMF} and sunspot number in the period covering cycles 20–22. However, it can be seen that the B_{HMF}, during the minimum of cycle 23, went down well below the floor level of 4.6 nT and reached ~3.5 nT. Since the surviving polar fields or the small-scale solar magnetic fields during the solar minimum are thought to be the sources of slow solar wind flows (Cliver & Ling, 2011; Wang & Sheeley, 2013), which determine the floor level of the HMF, Cliver and Ling (2011) reported a revised floor level of 2.8 nT for HMF. Their estimation was based on the two correlations: one between the axial dipole moment (the absolute difference between the polar fields of the northern and southern hemispheres) and the HMF at cycle minimum. The other between the HMF at cycle minimum of preceding cycles and the SSN_{max} of the following cycles. They used the data for the period covering cycles 14–23. Cliver and Herbst (2018) discussed the recent developments in the floor of HMF and reported that the floor level could have gone well below around 1.5 nT during the Maunder minimum period. Further, it is interesting to note, as seen from Figure 3c that, in cycle 24, the B_{HMF} by the year 2018 has already approached the value of the floor level of 4.6 nT about 2 years prior to the minimum of cycle 24. Thus, it is expected that we could witness the floor level of HMF also going down below the proposed floor level of 4.6 nT in cycle 24. Figure 3d plots the SSN V2.0 observations as a function of time for the period February 1975–December 2017, covering solar cycles 21–24. As mentioned earlier, a global reduction of SSN since cycle 21 up to cycle 24 is evident from Figure 3d.

Since the HMF results from solar photospheric fields being swept out into the inner heliosphere and beyond, the declining B_p beginning around mid-1990s during solar cycle 22, and continuing during cycles 23 and 24, would have contributed to the observed global reduction in the B_{HMF} and the reduction in the floor level of HMF during cycles 23 and 24. A plot of B_{HMF} versus B_p for the period February 1975–December 2017 is shown in Figure 4a. It is evident from Figure 4 that the B_{HMF} values post-1995 (filled red dots) show a clear reduction in their strength as compared to the values prior to 1995 (filled black dots). We found a moderate value of $r = 0.4$ at a confidence level of $P = 99\%$. The correlation was verified using the null hypothesis of a *t*-test statistics, and we found that the correlation is statistically significant. The values of *r*,*P* and *n* are indicated at the top left corner of Figure 4a. The solid black line in Figure 4a is a best fit to all the data points between B_{HMF} and B_p. The linear correlation of B_{HMF} and B_p is thus represented by the following equation,

$$B_{HMF} = 4.17 \pm (0.2) + (2.26 \pm 0.2) \times B_p \quad (2)$$

which gives an intercept of 4.17 (±0.2) nT for B_{HMF} when $B_p = 0$. This implies that the floor level of the HMF would be 4.17 nT even if solar polar field drops to zero. We, thus, see a reduced floor value of 4.17 nT for HMF (dash-dotted red line in Figure 4a), unlike the proposed floor level of 4.6 nT by Svalgaard and Cliver (2007) (solid blue line in Figure 4a), from a correlation of B_{HMF} and B_p for the period covering solar cycles 21–24. The reduced floor value of HMF is presumably due to the observed global reduction of the B_{HMF} post-1995. This reduced floor value of HMF is higher than the floor level of HMF of 2.8 nT proposed by Cliver and Ling (2011) (dashed black line in Figure 4a). It is to be noted here that Cliver and Ling (2011) used the correlation of HMF and dipole moment (the signed PMF) at solar minima to compute the floor value of 2.8 nT.

We now thus consider the correlation of B_{HMF} and B_p only during solar minima as reported in JBA15 which is also shown in Figure 4b. This is based on the fact that solar polar fields provide most of the HMF during

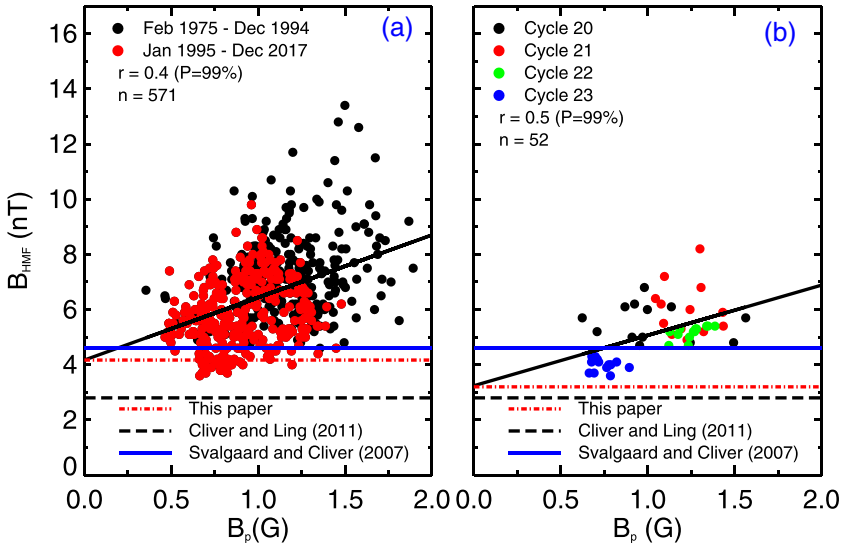

Figure 4. (a) B_{HMF} as function of B_p shown for the period February 1975–December 2017 covering solar cycles 21–24. The filled black and red dots in panel (a) are measurements for the period February 1975–December 1994 and January 1995–December 2017, respectively. (b) B_{HMF} as function of B_p shown for 1 year interval during the minima of cycles 20–23. The filled dots in different colors represent measurements for each solar cycle, from cycles 20–23. The solid black lines in both the panels are overall fits to the respective data points covering the cycles 21–24 and the minima of cycles 20–23. The respective values of $r = 0.4$ and 0.5 are indicated in the top left corners of the panels. The solid blue and dashed black lines in both panels indicate the floor levels of HMF of 4.6 and 2.8 nT as computed by Svalgaard and Cliver (2007) and Cliver and Ling (2011), respectively, while the dash-dotted lines indicate the floor levels of 4.2 and 3.2 nT, respectively, as obtained in this study.

solar minimum (Svalgaard et al., 2005). The overall fit to all data points between cycles 20–23 is shown by a solid black line in Figure 4b with an intercept of 3.2 (±0.5) nT for the HMF when B_p would go to zero and represented by the equation

$$B_{HMF} = 3.2 \pm (0.5) + (1.81 \pm 0.45) \times B_p \quad (3)$$

The floor level of HMF is thus, ~3.2 nT indicated by a dash-dotted red line in Figure 4b, a value that has dropped by more than 1 nT from the proposed floor level of 4.6 nT. It is to be noted that the value of ~3.2 nT is within 1σ uncertainty of the revised floor level of 2.8 nT (dashed balck line in Figure 4b) reported by Cliver and Ling (2011). This reduction in the floor of HMF could also be due to the reduced HMF during solar cycles 23 and 24. Thus, in order to show the contribution of the reduced HMF (due to declining B_p since the mid-1990s), we have plotted B_{HMF} versus B_p shown by filled dots of different colors for each solar cycle in Figure 4b. It is evident from Figure 4b that the values of B_{HMF} are above the floor level of 4.6 nT for the minima of cycles 20–22. However, the values of B_{HMF} (filled blue dots in Figure 4b) have gone below the floor level of 4.6 nT during the minimum of cycle 23, and so we see the reduction in the floor level of HMF down to 3.2 nT. As stated earlier, one could expect B_{HMF} during the upcoming minimum of cycle 24 to go below the floor level of 4.6 nT. Also, as already we had seen a value of HMF of 3.5 nT during the minimum of cycle 23, the floor level of B_{HMF} during the minimum of cycle 24 could be well around 3.2 nT. We have thus used Equation 3 and the value of B_p of 0.51 G in order to obtain a value of B_{HMF} of 4.17 (±0.7) nT at 2020. The previous estimated value of B_{HMF} in 2020 obtained in JBA15 was 3.9 (±0.6) nT. If on the other hand the minimum of solar cycle 24 occurs in 2021, then B_{HMF} in 2021 would be 4.12 (±0.7) nT.

3.3. Amplitude of Solar Cycle 25

The correlation between B_{min} of preceding cycles and SSN_{max} of following cycles is shown in Figure 5. Figures 5a and 5b, respectively, show the correlations obtained using SSN V1.0 and V2.0 observations. The values of B_{min} used in this study are from Cliver and Ling (2011) (see Table 2 in Cliver & Ling, 2011). The respective values of $r = 0.80$ (for V1.0) and 0.76 (for V2.0) at a confidence level of $P = 99\%$ are indicated at the top right corner of each panel. The correlation between B_{min} and SSN_{max} for SSN V1.0 is given by

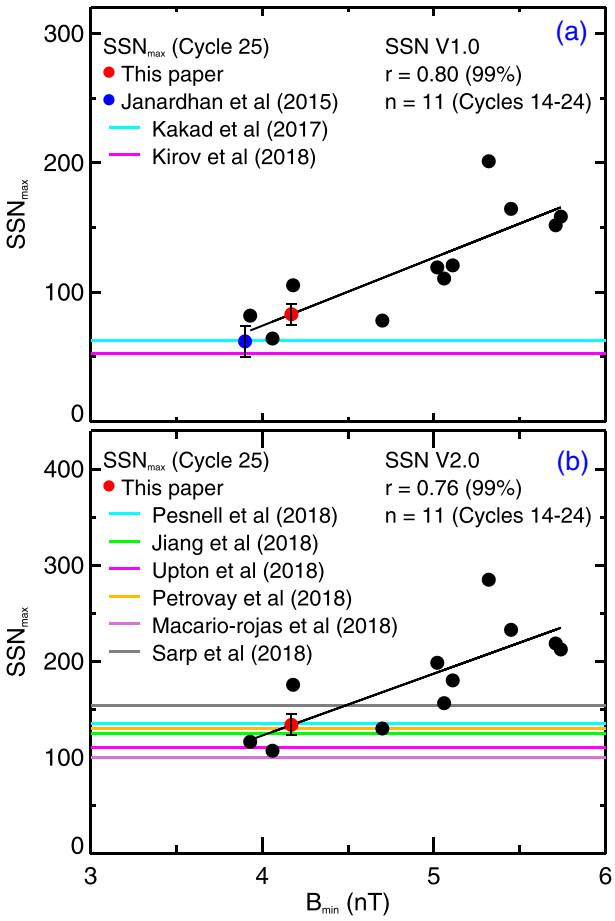

Figure 5. (a) SSN_{max} of following cycles from cycles 14–24 as a function of B_{min} of preceding cycles from cycles 13–23 shown for SSN V1.0 (b) the same for SSN V2.0. The filled black dots with solar cycle numbers in each panel are the values of SSN_{max} as function of B_{min} for each solar cycle from cycles 14–24, while the solid black line in each panel is a best fit line to all data points from cycles 14–24. The predictions for cycle 25 obtained by different researchers and this study are indicated by horizontal lines, solid red, and blue dots as indicated by the legends in each panel.

$$SSN_{max} = 52.6(\pm 12.9) \times B_{min} - 136.5(\pm 64) \quad (4)$$

Using the value of B_{min} of 3.9 nT for cycle 24 in Equation 1, JBA15 derived a SSN_{max} of 62 ± 12 for cycle 25, indicated by a solid blue dot in Figure 5a. Using the updated value of B_{min} of 4.17 nT for cycle 24 (see section 3.2) in Equation 4, we predict a SSN_{max} of 83 ± 8 for cycle 25. This value is indicated by a solid red dot with 1 sigma error bar in Figure 5a. Similarly if solar minimum of cycle 24 occurs in 2021, the updated SSN_{max} on the SSN V1.0 scale would be 80 ± 8. It is, thus, seen that the prediction using the SSN V1.0 observations indicate a cycle 25 similar to cycle 24 which had a SSN_{max} of 81.9. The two other predictions, using SSN V1.0 observations, made by Kakad et al. (2017) and Kirov et al. (2018), have been indicated by the colored horizontal lines in Figure 5a, that claimed too a cycle 25 similar to cycle 24.

On the other hand, the correlation between B_{min} and SSN_{max} for SSN V2.0 data is given by

$$SSN_{max} = 64.4(\pm 17.9) \times B_{min} - 134.8(\pm 89) \quad (5)$$

Using the value of B_{min} of 4.17 nT for cycle 24 in Equation 5, we predict a SSN_{max} of 134 ± 11 for cycle 25 if the solar minimum is in 2020. This is shown by a solid red dot with 1 sigma error bar in Figure 5b with the differently colored horizontal lines indicating predictions for cycle 25 by other researchers, using SSN V2.0 observations. The ratio of the values of SSN_{max} predicted for cycle 25 to the values of SSN_{max} for cycle 24 by these authors has been given in Table 1. It is already clear from both Table 1 and from Figure 5b as to why Upton and Hathaway (2018) and Macario-Rojas et al. (2018) argued for a solar cycle 25 that would be more or less like solar cycle 24. In contrast, the prediction reported in this study using SSN V2.0 observations with a SSN_{max} of 134 ± 11 for cycle 25 suggests a stronger cycle 25 than cycle 24, which had a SSN_{max} of 116. Similarly the updated SSN_{max} for cycle 25 is 131 ± 11 if solar minimum of cycle 24 happens in 2021 suggesting also an upcoming cycle 25 stronger than cycle 24. Our prediction, in fact, agrees with the predictions made by Jiang et al. (2018), Pesnell and Schatten (2018), and Petrovay et al. (2018) who claimed a similar result for the amplitude of cycle 25.

4. Discussion and Conclusions

Our study reports the temporal changes in SPF obtained from NSO/KP and NSO/SOLIS synoptic magnetograms, covering solar cycles 21 – 24, specifically paying attention to the manner in which the unsigned PMF at latitudes ≥45° behaved after the mini solar maximum of cycle 24. In the present study, it has been shown that after the solar maximum of cycle 24, unexpectedly, there has been an increase in the unsigned PMF strength in the year 2015 that has subsequently shown a slow and steady change maintaining the declining trend, that had begun around the mid-1990s, for more than about 22 years. Importantly, it appears that the unsigned PMF have switched their correlation with solar cycle activity behavior in cycles 21 and 22 to anti-correlation with solar cycle activity behavior in cycle 24 and showing no correlation with sunspot cycle in between, suggesting a transition phase of solar magnetic fields during cycle 23.

As per the current understanding of the solar dynamo process that gives rise to the solar cycle and as proposed by solar dynamo models (Charbonneau, 2010), sunspot or toroidal fields are generated from poloidal fields by solar differential rotation, while poloidal or polar fields are regenerated from toroidal fields by the Babcock-Leighton mechanism (Babcock, 1961; Leighton, 1969). This mechanism depends on the systematic tilt angle distribution of bipolar sunspot regions, which, in turn, is determined by the Coriolis force acting on the magnetic flux tubes that rise through the solar surface at different latitudes to produce bipolar sunspot

regions (D'Silva & Choudhuri, 1993). This whole process would result in a large scatter in tilt angle distribution, which, along with diffusion and surface flux transport processes, could change the solar polar field behavior in any given solar cycle, thereby making it totally different from the previous cycle. The sudden transition of behavior of unsigned PMF in cycle 24 can, thus, be attributed to the fluctuations in Babcock-Leighton mechanism that decide the net flux transported toward the poles and, thereby, ultimately determining the net polar field strength at the end of a cycle.

We have re-estimated, in this study, the average field strength of ~2.1 G for the unsigned PMF in 2020 for the upcoming solar minimum of cycle 24. Also, using the correlation between the strength of HMF and the unsigned PMF during the minima of cycles 20–23, we have re-estimated a value of 4.17 nT for the HMF in 2020. Further, based on the correlation of HMF of previous solar minima and SSN_{max} of following solar maxima from cycles 14–24, we estimated a value of SSN_{max} of 83 ± 8 (V1.0) and 134 ± 11 (V2.0) for the upcoming solar cycle 25. Expecting a delay in the minimum of cycle 24 by 1 year, that is, 2021, we also estimated a value of SSN_{max} of 80 ± 8 (V1.0) and 131 ± 11 (V2.0) for the upcoming solar cycle 25. Our estimate of SSN_{max} (V2.0) suggests that the oncoming sunspot cycle 25 will be stronger than cycle 24 but will be weaker than cycles 23. The stronger upcoming cycle 25 can be understood from the fact that the axial dipole moment during cycle 24 (by December 2017) has been stronger than that during cycle 23 (Jiang et al., 2018). This is in keeping with the flux transport dynamo model by Choudhuri et al. (2007) wherein the authors predicted a weaker cycle 24 based on the weaker axial dipole moment during cycle 23.

Using the values of solar spectral irradiance at 10.7 cm (F10.7) and the averaged polar magnetic field, Pesnell and Schatten (2018) computed a solar dynamo amplitude (SODA) index. They used the SODA index as a precursor for predicting the next cycle's amplitude and estimated a maximum SSN V2.0 of 135 ± 25 for cycle 25. The Fe XIV coronal green line emission appears at high latitudes (≥50°) just before solar cycle maximum, which subsequently drifts to the poles. This is known as rush-to-the-poles (RTTP). Based on the correlations of the rise rate of the RTTP to the delay time between the end of the RTTP and the maximum of the following cycle, Petrovay et al. (2018) estimated the maximum SSN V2.0 of cycle 25 of 130. Similarly, using the surface flux transport model Jiang et al. (2018) predict the polar field strength at the end of cycle 24 and predicted the amplitude of cycle 25 to be 125 ± 32, indicating a 10% stronger cycle 25 than cycle 24. Also, using continuous century-scale data-driven surface flux transport simulations, Bhowmik and Nandy (2018) reported a slightly stronger solar cycle 25 than cycle 24 with a SSN_{max} ranging between 109 and 139 (V2.0). Thus, using the revised SSN V2.0 and the other existing correlations that relate to the strength of the following cycle, the other researchers also arrived at the same conclusion for the amplitude of cycle 25 similar to the stronger cycle 25 as proposed by this study.

With space missions like the Parker Solar Probe being operational and upcoming solar missions like the ADITYA-L1 mission, by India, planned for launch in 2020 (Janardhan et al., 2017), cycle 25 is bound to reveal more crucial insights into as yet unknown aspects of the internal workings of our Sun.

Data Availability Statement

Photospheric magnetic field data used in this study are obtained from NSO/KP and NSO/SOLIS magnetogram data base that are available at https://www.nso.edu/data/dataset/ and https://solis.nso.edu/0/vsm/vsm_maps.php, respectively. The method to extract photospheric magnetic field data from magnetogram is explained in detail in Janardhan et al. (2018). Polar field data used from Wilcox Solar Observatory are available online (https://wso.stanford.edu/Polar.html). While the heliospheric magnetic field data used are available at the OMNI2 database (https://omniweb.gsfc.nasa.gov/). Smoothed sunspot number data used for version 1.0 and 2.0 are obtained online (https://www.sidc.be/silso/datafiles).

Acknowledgments

This work has made use of NASA's OMNIWEB services Data System. The authors thank the free data use policy of the National Solar Observatory (NSO/KP and NSO/SOLIS), OMNI2 from NASA and WDC-SILSO at Royal Observatory, Belgium, Brussels. S. K. B. acknowledges the support by the PIFI (Project No. 2015PM066) program of the Chinese Academy of Sciences and the NSFC (Grants 11750110422, 11433006, 11790301, and 11790305). S. A. acknowledges an INSA Honorary Scientist position. We thank the reviewers for their constructive and thorough comments that help us to improve the paper significantly.

References

Babcock, H. W. (1961). The topology of the Sun's magnetic field and the 22-year cycle. *The Astrophysical Journal*, *133*, 572. https://doi.org/10.1086/147060

Bhowmik, P., & Nandy, D. (2018). Prediction of the strength and timing of sunspot cycle 25 reveal decadal-scale space environmental conditions. *Nature Communications*, *9*, 5209. https://doi.org/10.1038/s41467-018-07690-0

Bisoi, S. K., Janardhan, P., Chakrabarty, D., Ananthakrishnan, S., & Divekar, A. (2014). Changes in quasi-periodic variations of solar photospheric fields: Precursor to the deep solar minimum in cycle 23?. *Solar Physics*, *289*, 41–61. https://doi.org/10.1007/s11207-013

Cameron, R. H., Jiang, J., & Schüssler, M. (2016). Solar cycle 25: Another moderate cycle? *The Astrophysical Journal Letters*, *823*, L22. https://doi.org/10.3847/2041-8205/823/2/L22

Charbonneau, P. (2010). Dynamo models of the solar cycle. *Living Reviews in Solar Physics*, *7*, 3. https://doi.org/10.12942/lrsp-2010-3
Choudhuri, A. R., Chatterjee, P., & Jiang, J. (2007). Predicting solar cycle 24 with a solar dynamo model. *Physical Review Letters*, *98*(13), 131,103. https://doi.org/10.1103/PhysRevLett.98.131103
Choudhuri, A. R., & Karak, B. B. (2012). Origin of grand minima in sunspot cycles. *Physical Review Letters*, *109*(17), 171,103. https://doi.org/10.1103/PhysRevLett.109.171103
Clette, F., & Lefèvre, L. (2016). The new sunspot number: Assembling all corrections. *Solar Physics*, *291*, 2629–2651. https://doi.org/10.1007/s11207-016-1014-y
Cliver, E. W. (2016). Comparison of new and old sunspot number time series. *Solar Physics*, *291*, 2891–2916. https://doi.org/10.1007/s11207-016-0929-7
Cliver, E. W., & Herbst, K. (2018). Evolution of the sunspot number and solar wind B time series. *Space Science Reviews*, *214*(2), 56. https://doi.org/10.1007/s11214-018-0487-4
Cliver, E. W., & Ling, A. G. (2011). The floor in the solar wind magnetic field revisited. *Solar Physics*, *274*, 285–301. https://doi.org/10.1007/s11207-010-9657-6
D'Silva, S., & Choudhuri, A. R. (1993). A theoretical model for tilts of bipolar magnetic regions. *Astronomy & Astrophysics*, *272*, 621.
de Toma, G. (2011). Evolution of coronal holes and implications for high-speed solar wind during the minimum between cycles 23 and 24. *Solar Physics*, *274*, 195–217. https://doi.org/10.1007/s11207-010-9677-2
Gopalswamy, N., Mäkelä, P., Yashiro, S., & Akiyama, S. (2018). Long-term solar activity studies using microwave imaging observations and prediction for cycle 25. *Journal of Atmospheric and Solar-Terrestrial Physics*, *176*, 26–33. https://doi.org/10.1016/j.jastp.2018.04.005
Gopalswamy, N., Yashiro, S., & Akiyama, S. (2016). Unusual polar conditions in solar cycle 24 and their implications for cycle 25. *The Astrophysical Journal Letters*, *823*, L15. https://doi.org/10.3847/2041-8205/823/1/L15
Gopalswamy, N., Yashiro, S., Mäkelä, P., Michalek, G., Shibasaki, K., & Hathaway, D. H. (2012). Behavior of solar cycles 23 and 24 revealed by microwave observations. *The Astrophysical Journal Letters*, *750*, L42. https://doi.org/10.1088/2041-8205/750/2/L42
Hathaway, D. H., & Upton, L. A. (2016). Predicting the amplitude and hemispheric asymmetry of solar cycle 25 with surface flux transport. *Journal of Geophysical Research: Space Physics*, *121*, 10,744–10,753. https://doi.org/10.1002/2016JA023190
Iijima, H., Hotta, H., Imada, S., Kusano, K., & Shiota, D. (2017). Improvement of solar-cycle prediction: Plateau of solar axial dipole moment. *Astronomy & Astrophysics*, *607*, L2. https://doi.org/10.1051/0004-6361/201731813
Ingale, M., Janardhan, P., & Bisoi, S. K. (2019). Beyond the mini-solar maximum of solar cycle 24: Declining solar magnetic fields and the response of the terrestrial magnetosphere. *Journal of Geophysical Research: Space Physics*, *124*, 6363–6883. https://doi.org/10.1029/2019JA026616
Janardhan, P., Bisoi, S. K., Ananthakrishnan, S., Tokumaru, M., Fujiki, K., Jose, L., & Sridharan, R.(2015). A 20 year decline in solar photospheric magnetic fields: Inner-heliospheric signatures and possible implications. *Journal of Geophysical Research: Space Physics*, *120*, 5306–5317. https://doi.org/10.1002/2015JA021123
Janardhan, P., Bisoi, S. K., & Gosain, S. (2010). Solar polar fields during cycles 21–23: Correlation with meridional flows. *Solar Physics*, *267*, 267–277. https://doi.org/10.1007/s11207-010-9653-x
Janardhan, P., Fujiki, K., Ingale, M., Bisoi, S. K., & Rout, D. (2018). Solar cycle 24: An unusual polar field reversal. *Astronomy & Astrophysics*, *618*, A148. https://doi.org/10.1051/0004-6361/201832981
Janardhan, P., Vadawale, S. V., Bapat, B., Subramanian, K. P., Chakrabarty, D., Kumar, P., et al. (2017). Probing the heliosphere using in-situ payloads on-board Aditya-L1. *Current Science*, *113*, 620–624. https://doi.org/10.18520/cs/v113/i04/620-624
Jiang, J., Wang, J.-X., Jiao, Q.-R., & Cao, J.-B. (2018). Predictability of the solar cycle over one cycle. *The Astrophysical Journal*, *863*, 159. https://doi.org/10.3847/1538-4357/aad197
Kakad, B., Kakad, A., & Ramesh, D. S. (2017). Shannon entropy-based prediction of solar cycle 25. *Solar Physics*, *292*, 95. https://doi.org/10.1007/s11207-017-1119-y
Karak, B. B., & Choudhuri, A. R. (2013). Studies of grand minima in sunspot cycles by using a flux transport solar dynamo model. *Research in Astronomy & Astrophysics*, *13*, 1339–1357. https://doi.org/10.1088/1674-4527/13/11/005
Kirov, B., Asenovski, S., Georgieva, K., Obridko, V. N., & Maris-Muntean, G. (2018). Forecasting the sunspot maximum through an analysis of geomagnetic activity. *Journal of Atmospheric and Solar-Terrestrial Physics*, *176*, 42–50. https://doi.org/10.1016/j.jastp.2017.12.016
Komm, R., Howe, R., & Hill, F. (2018). Subsurface zonal and meridional flow during cycles 23 and 24. *Solar Physics*, *293*, 145. https://doi.org/10.1007/s11207-018-1365-7
Leighton, R. B. (1969). A magneto-kinematic model of the solar cycle. *The Astrophysical Journal*, *156*, 1. https://doi.org/10.1086/149943
Macario-Rojas, A., Smith, K. L., & Roberts, P. C. E. (2018). Solar activity simulation and forecast with a flux-transport dynamo. *Monthly Notices of the Royal Astronomical Society*, *479*, 3791–3803. https://doi.org/10.1093/mnras/sty1625
Miyahara, H., Kitazawa, K., Nagaya, K., Yokoyama, Y., Matsuzaki, H., Masuda, K., et al. (2010). Is the Sun heading for another Maunder minimum? - Precursors of the grand solar minima. *Journal of Cosmology*, *8*, 1970–1982.
Muñoz-Jaramillo, A., Sheeley, N. R., Zhang, J., & DeLuca, E. E. (2012). Calibrating 100 years of polar faculae measurements: Implications for the evolution of the heliospheric magnetic field. *The Astrophysical Journal*, *753*, 146. https://doi.org/10.1088/0004-637X/753/2/146
Pesnell, W. D. (2018). Effects of version 2 of the international sunspot number on naïve predictions of solar cycle 25. *Space Weather*, *16*, 1997–2003. https://doi.org/10.1029/2018SW002080
Pesnell, W. D., & Schatten, K. H. (2018). An early prediction of the amplitude of solar cycle 25. *Solar Physics*, *293*, 112. https://doi.org/10.1007/s11207-018-1330-5
Petrovay, K., Nagy, M., Gerják, T., & Juhász, L. (2018). Precursors of an upcoming solar cycle at high latitudes from coronal green line data. *Journal of Atmospheric and Solar-Terrestrial Physics*, *176*, 15–20. https://doi.org/10.1016/j.jastp.2017.12.011
Sánchez-Sesma, J. (2016). Evidence of cosmic recurrent and lagged millennia-scale patterns and consequent forecasts: Multi-scale responses of solar activity (SA) to planetary gravitational forcing (PGF). *Earth System Dynamics*, *7*, 583–595. https://doi.org/10.5194/esd-7-583-2016
Sarp, V., Kilcik, A., Yurchyshyn, V., Rozelot, J. P., & Ozguc, A. (2018). Prediction of solar cycle 25: A non-linear approach. *Monthly Notices of the Royal Astronomical Society*, *481*, 2981–2985. https://doi.org/10.1093/mnras/sty2470
Sasikumar Raja, K., Janardhan, P., Bisoi, S. K., Ingale, M., Subramanian, P., Fujiki, K., & Maksimovic, M. (2019). Global solar magnetic field and interplanetary scintillations during the past four solar cycles. *Solar Physics*, *294*, 123. https://doi.org/10.1007/s11207-019-1514-7
Sun, X., Hoeksema, J. T., Liu, Y., & Zhao, J. (2015). On polar magnetic field reversal and surface flux transport during solar cycle 24. *The Astrophysical Journal*, *798*, 114. https://doi.org/10.1088/0004-637X/798/2/114
Svalgaard, L., & Cliver, E. W. (2007). A floor in the solar wind magnetic field. *The Astrophysical Journal Letters*, *661*, L203–L206. https://doi.org/10.1086/518786

Svalgaard, L., Cliver, E. W., & Kamide, Y. (2005). Sunspot cycle 24: Smallest cycle in 100 years?. *Geophysical Research Letters*, *32*, L01104. https://doi.org/10.1029/2004GL021664

Upton, L., & Hathaway, D. H. (2014). Predicting the Sun's polar magnetic fields with a surface flux transport model. *The Astrophysical Journal*, *780*, 5. https://doi.org/10.1088/0004-637X/780/1/5

Upton, L. A., & Hathaway, D. H. (2018). An updated solar cycle 25 prediction with AFT: The modern minimum. *Geophysical Research Letters*, *45*, 8091–8095. https://doi.org/10.1029/2018GL078387

Usoskin, I. G., Solanki, S. K., & Kovaltsov, G. A. (2007). Grand minima and maxima of solar activity: New observational constraints. *Astronomy & Astrophysics*, *471*, 301–309. https://doi.org/10.1051/0004-6361:20077704

Wang, Y.-M., Robbrecht, E., & Sheeley, N. R. (2009). On the weakening of the polar magnetic fields during solar cycle 23. *The Astrophysical Journal*, *707*, 1372–1386. https://doi.org/10.1088/0004-637X/707/2/1372

Wang, Y.-M., & Sheeley, N. R. (2013). The solar wind and interplanetary field during very low amplitude sunspot cycles. *The Astrophysical Journal*, *764*, 90. https://doi.org/10.1088/0004-637X/764/1/90

Zachilas, L., & Gkana, A. (2015). On the verge of a grand solar minimum: A second Maunder minimum? *Solar Physics*, *290*, 1457–1477. https://doi.org/10.1007/s11207-015-0684-1

Zolotova, N. V., & Ponyavin, D. I. (2014). Is the new grand minimum in progress?. *Journal of Geophysical Research: Space Physics*, *119*, 3281–3285. https://doi.org/10.1002/2013JA019751